Multidisciplinary Materials Chronicles, 2025, Vol. 2, Iss. 1, 92-103

DOI: 10.62184/mmc.jmmc110020254

Research Article

SCIENCE PARK PUBLISHER

Multidisciplinary Materials Chronicles

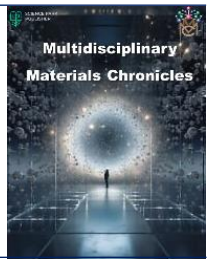

Enhancing thermal and mechanical properties of aluminum composites through high-entropy alloy reinforcement

Alqasem M. Alsamawi[1,*], Essam B. Moustafa[1,2] , Ahmed B. Khoshaim[1]

[1] Department of Mechanical Engineering, King Abdulaziz University, Jeddah, 22254, Saudi Arabia

[2] Benha National University, Faculty of Engineering, Egypt

Received: 04, 03, 2025; Accepted: 11, 04, 2025; Published: 27, 04, 2025

Abstract

This study investigates the thermal and mechanical properties of pure aluminum composites reinforced with varying weight percentages (5-30 wt%) of high-entropy alloy (HEA) (Fe-Co-Ni- Cr-Mo). The composites were fabricated using powder metallurgy techniques, and their thermal expansion behavior was analyzed at room temperature to 400 °C. The results demonstrate a significant reduction in the coefficient of thermal expansion (CTE) with increasing HEA content, achieving a 39% decrease at 30 wt% HEA compared to pure aluminum. This enhancement is attributed to forming a stable, interconnected HEA network within pure aluminum, effectively restricting thermal expansion. Modal and buckling analyses further reveal improved mechanical properties, including increased resonance frequencies and enhanced structural stability, with increasing HEA reinforcement. The findings highlight the potential of tailoring aluminum composites with specific thermal and mechanical properties for advanced engineering applications by controlling the HEA content.

Keywords: Thermal behavior, Mechanical Properties, High-Entropy Alloy, Reinforcement, Aluminum

1. Introduction

Recently, a new class of metallic materials with an orbital arrangement was discovered, which has properties between its constitutive substances. They were named HEAs or multi-principal-element alloys [1-3]. Composite materials are beneficial in engineering applications and have been proven by society for a long time. Aluminum and its alloys have high strength-to-weight ratios, excellent castability and plastic deformation, and resistance to mild to moderate alkali corrosion [4-6]. They are promising matrix materials for manufacturing metal matrix composites. HEAs contain four or more components with nearly equal molar percentages and crystal structures [7, 8]. HEAs, or instead using a broader term, the multi-principal-element alloys (MPEAs), have at least five principal elements, present a serene structure, and feel the influence of entropy in governing the atomic configurations, leading to potential high strength and excellent ductility [8, 9]. In volume corporally, scarcely any defective dislocations are generated due to the pile-up of single-element metallic solid solutions and also through the twin boundaries in MPEAs [10]. These most elongated, disordered, and robust microstructures help to enhance the resistance to plastification. In addition to strengthening mechanisms, MPEAs show enormous potential as healing and passivation inductors that can improve damage tolerance. This is attributed to the significant and low-uniform mechanical and thermal maturity of these elements in as-cast and heat-treated multiphasic MPEAs, which enables a combination of Pop-I and II accident toughness to be developed [11].

Multidisciplinary Materials Chronicles, 2025, Vol. 2, Iss. 1, 92-103
DOI: 10.62184/mmc.jmmc110020254

Research Article

The thermal behavior and properties of single high-entropy alloys and bulk materials are stated. Materials with crystalline structures play a part in the lattice entropy compared to amorphous solids [12-15]. Adding one or two more elements could raise the glass transition and crystallization temperatures. Moreover, the glass transition, crystallization temperature, and supercooling were improved by increasing the amounts of the parameter in the $Fe_{17}Cr_{27}Ni_{26}Mo_5Al_{0.5}RE_2MPCo_4Ga$ HEA glassy coatings [16, 17]. However, few researchers have improved the thermal properties of alloys by adding interference solid solutions to overcome fast crystallization [18]. Based on the discussion, a question arises regarding the common physical properties and applications of high-entropy alloys in practice. Suppose the array of sub-microscopic regions of the pasty and solid structure based on high-alloy elements is essential. In that case, they can reinforce particles in metals and alloys [19-22].

The time dependency of the thermal properties of semicrystalline polymers can be treated to determine their thermal properties based on the equation, analyzing non-isothermal X-ray diffraction results and constant heating rate experiments [23, 24]. The study sets different percentages of compositions: 5 and 10 wt%. Composite materials were formed to enlarge the surface heat of the entrance on produced test plates [25]. The study shows the differences in the thermal conductivity of composites depending on the composition of sprayed particles used in the manufacturing process [26]. Very little research exists on the reinforcement of aluminum using the HEM discussed earlier. Simulation research of the HEM in aluminum has not been done [27, 28]. This also shows how unexplored research is related to modifying thermal properties through alloying. Limited research has been conducted based on experimental and simulation analysis of Al/Fe-Co-Ni-Cr-Mo for varying concentrations by reinforcing aluminum. This paper aims to study the thermal presentation of aluminum/Fe-Co-Ni-Cr-Mo HEAs composites produced by the addition of more high entropy alloy from the critical composition to the limit one by 5%, 10,15,20%, 25%, and 30% by weight in the pure aluminum under the categories of thermal transport (thermal diffusivity and thermal conductivity). This research is of significant importance from both academic and practical perspectives. Understanding and knowledge of this type of material and its correlation properties are wholly needed in emerging technologies and in producing developed composites. The commercial composite was adjusted to match the percentage of high entropy. The experimental results showed that increasing the high entropy alloy enhanced the thermal properties. In recent years, scientific research has witnessed accelerated development in the manufacturing and application of HEA, expanding their utilization across diverse industrial domains. For example, Sonar et al. discuss aerospace applications: Recent progress of high-entropy alloys and their applications in aero-engine components [7]. Kareem et al. provide a detailed analysis of thermal management applications through their comprehensive review of electronic and thermal management: Aluminum matrix composites reinforced with high entropy alloys [8]. Automotive and structural applications research progress on multi-component alloying by Zhang et al. discusses automotive applications [4]. Also, manufacturing and industrial applications: Challenges in additive manufacturing of high-strength aluminum alloys are discussed by Altıparmak et al. [6].

2. Experimental work

2.1. Powder metallurgy techniques

Pure aluminum was selected as the matrix material, and various pure aluminum was chosen for reinforcement. Additionally, a high entropy alloy (HEA) with the equiatomic composition Fe-Co-Ni-Cr-Mo was utilized as a reinforcing phase at various weight percentages (5%, 10%, 15%, 20%, 25%, and 30%). Powder metallurgy techniques were employed to fabricate the aluminum-based composites with varying HEA content. Nonreactive powder mixing followed by three hours of planetary mechanical milling was conducted to ensure a homogenous mixture and minimize interfacial discrepancies. A ball-to-powder ratio (BPR) of 18:1 was maintained during milling. Ethyl alcohol in dust form was used as the milling medium due to the high surface area of the fine powders, which presented a combustion risk. The final blended powder (BM) was sealed under an ultra-high-purity (UHP) argon atmosphere to prevent oxidation during processing. Milling was performed in a planetary ball mill at 1550 RPM for five hours using 12 mm stainless steel balls and 5 mm steel balls with 18 g of aluminum powder. The distribution of HEA in the pure aluminum was determined using equation (1):

$$xAl = mAl / (mAl + mHEA) \quad (1)$$

where:

- xAl represents the weight fraction of the pure aluminum in the composite.

Multidisciplinary Materials Chronicles, 2025, Vol. 2, Iss. 1, 92-103

DOI: 10.62184/mmc.jmmc110020254

Research Article

- mAl is the mass of aluminum powder.
- mHEA is the mass of the HEA powder.

"BM" denotes the initial composite mixture before any reaction, while "PRE" refers to the composite after a 3-hour secondary milling stage. Material Preparation: Weight percentages of 5- 30 wt% HEA were precisely weighed using a Camry digital balance for pure aluminum powder and HEA (Fe-Co-Ni-Cr-Mo) powder. Reliably labeled plastic bags were employed for the storage of powders. A custom-made stainless steel die set was fabricated according to the specifications shown in Figure 1. The die set includes two punches and two dies. The coin size is 24.9 mm in diameter with an 8 mm thickness. Punch 1 has a diameter of 2.5 cm and a length of 3 cm, while the inner diameter, outer diameter, and thickness of the die are 25 mm, 70 mm, and 30 mm, respectively.

Figure 2 shows that the homogenized powder combination was re-evaluated for weight. Upon completion of all these stages, the die assembly was prepared. Initially, die number 1 and punch two were employed to secure the powder mixture, ensuring compaction for uniform distribution. The powder bed was then covered with die number one. Figure 2d illustrates the compaction process with a Metallkraft WPP 60 MBK hydraulic press. The pre-assembled die was accurately positioned and centered on the hydraulic press. Punch 1 was centrally aligned with die 2 to apply axial load. The compaction process was conducted at a pressure of 120 bar, with a tolerance of ±2 bar, and sustained for 10–15 seconds to achieve optimum densification of the green compact. The powder mixture was placed into the die cavity, and a hydraulic press was utilized to exert the compaction pressure. To ensure reproducibility, a standardized protocol was followed for all samples, including consistent powder loading, identical compaction pressure and duration, and uniform handling techniques by trained operators. Subsequently, as seen in Figure 2e, the green

specimens were removed from the die. The final weighing step was conducted to quantify material retention and assess any potential mass loss during the compaction process. The testing and sample preparation step encompassed the cleaning and measuring of the compacted samples. The materials were, after that, kept in sealed containers to prevent oxidation. Data was thoroughly categorized and documented for each composition. Creating samples ensured uniform quality across each while monitoring thermal expansion. The identical process is utilized to synthesize all compositions generated in HEA (5%, 10%, 15%, 20%, 25%, and 30%) to assess the influence of reinforcement content on thermal characteristics.

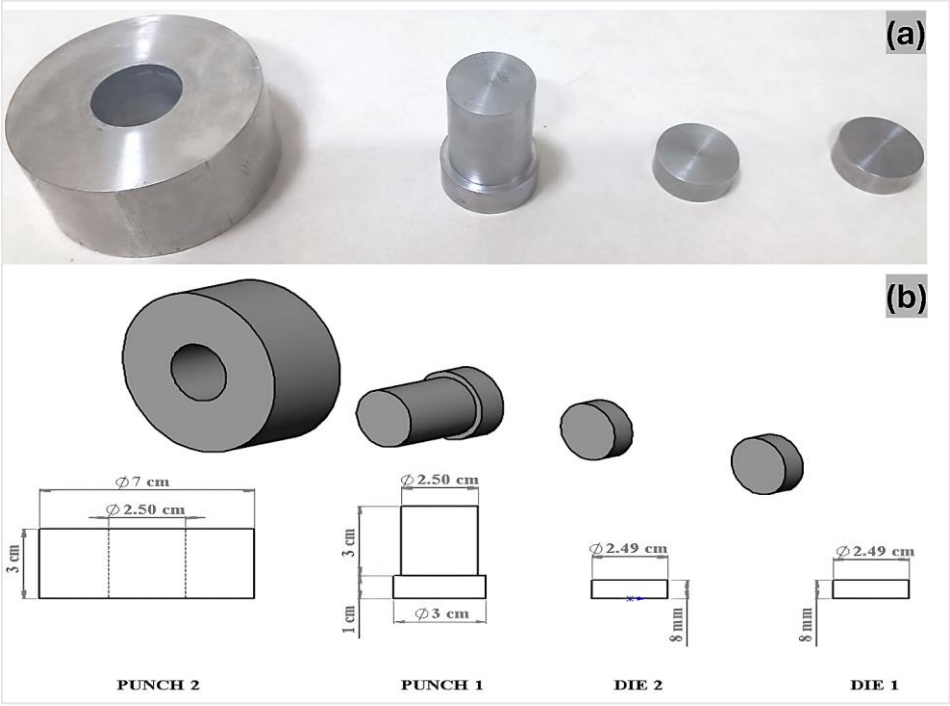

Figure 1. Components of the Custom Die-Punch Assembly for Powder Compaction **(a)** typical die components, **(b)** die design.

Multidisciplinary Materials Chronicles, 2025, Vol. 2, Iss. 1, 92-103

DOI: 10.62184/mmc.jmmc110020254

Research Article

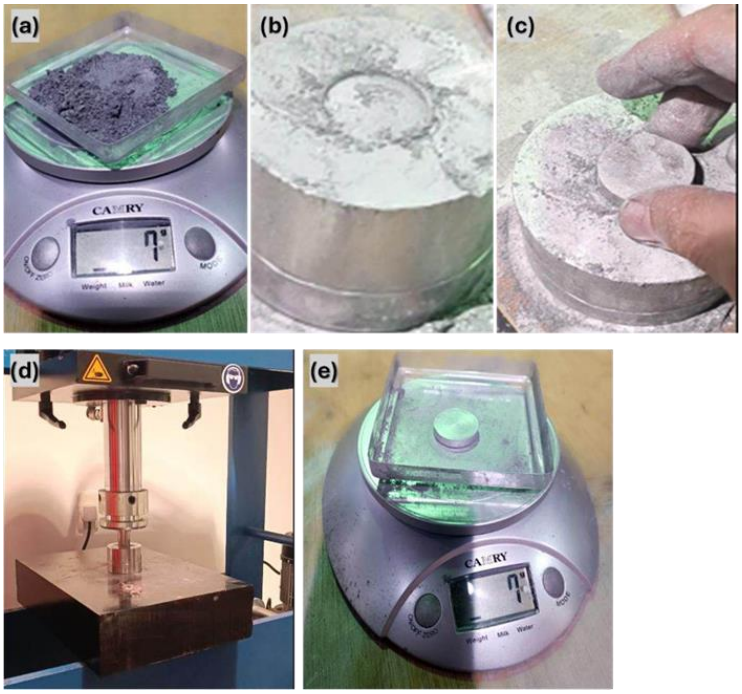

Figure 2. Process sequence for Al-HEA composite preparation and compaction: **(a)** Weighing of powder mixture using a digital balance, **(b)** Powder mixture preparation in the die cavity, **(c)** Manual handling and positioning of the powder compact, **(d)** WPP 60 MBK hydraulic press used for compaction at 120 bar, and **(e)** Final weighing of the compacted specimen.

2.2. Thermal expansion test

A vertical push-rod dilatometer system, which could measure dimensional changes at sub-micron level sensitivity, was utilized to characterize the thermal expansion behavior. Powder metallurgy methods produced cylindrical samples (diameter 24.9mm, length 8 mm). Samples were compressed using a Metallkraft hydraulic press (WPP 60 MBK) with custom-made stainless-steel die and punch assemblies. The system is called a dilatometer, and it contains a furnace chamber with programmable heating rates and controlled temperature, a Linear Variable Differential Transformer (LVDT) with high accuracy, and a Type-K thermocouple to ensure proper temperature detection. The data acquisition system recorded temperature and dimensional changes simultaneously. All measurements were performed at a heating rate of 5°C/min from room temperature to 400°C under a protective argon atmosphere to avoid and prevent oxidation. The thermal expansion was measured as d: ΔL/L (relative length change) as a function of temperature. The thermal expansion curves were fitted, and the coefficient of thermal expansion (CTE) was determined by fitting a line to the linear portion (25-400°C) of each thermal expansion curve.

2.3. Microstructure examination

To analyze the microstructure of aluminum-based composites reinforced with HEAs, SEM Scanning Electron Microscopy was employed. A TESCAN VEGA3 scanning electron microscope with a Schottky field emission source, operating at 30 kV accelerating voltage and achieving 1.5 nm resolution, was used for the analysis. The microscope was equipped with SE and BSE detectors, a digital imaging system, and energy-dispersive X-ray spectroscopy (EDS) for elemental analysis. Samples were examined in a high-vacuum environment to ensure superior image quality and accurate compositional analysis of the Al-HEA interfaces.

3. Results and discussions

3.1. Microstructural observations

Microstructural and thermal expansion analyses prove that Al's thermal property has been successfully modified by HEA reinforcement. Scanning electron microscopy reveals a pronounced change in microstructural features on the scale of

Multidisciplinary Materials Chronicles, 2025, Vol. 2, Iss. 1, 92-103
DOI: 10.62184/mmc.jmmc110020254

Research Article

experimental concentration for HEAs. Figure 3 shows results in a microstructure containing HEA as finely dispersed particles throughout pure aluminum for 5 wt% HEA occurring within micron-scale sizes. This distribution is indicative of efficient mechanical alloying and powder consolidation processes. In comparison, the more complex interconnected network of the 30 wt% HEA composite demonstrates better particle- particle contacts and better interfacial bond strength with the matrix. SEM micrographs (Figure 3) highlight the morphological changes from 5 wt% through to 30 wt% compositions of HEA. At 5 wt% HEA (Figure 3a), the microstructural given HEA particles are well dispersed, particularly if they produce non-uniform clusters, which are also typical of mechanical alloying values. The 30 wt% sample (Figure 3b) reveals a more homogeneous and linked HEA network structuring an increase in interparticle interactions. Schematic diagram of the structural evolution that directly affects the heat-transfer property of composites over time.

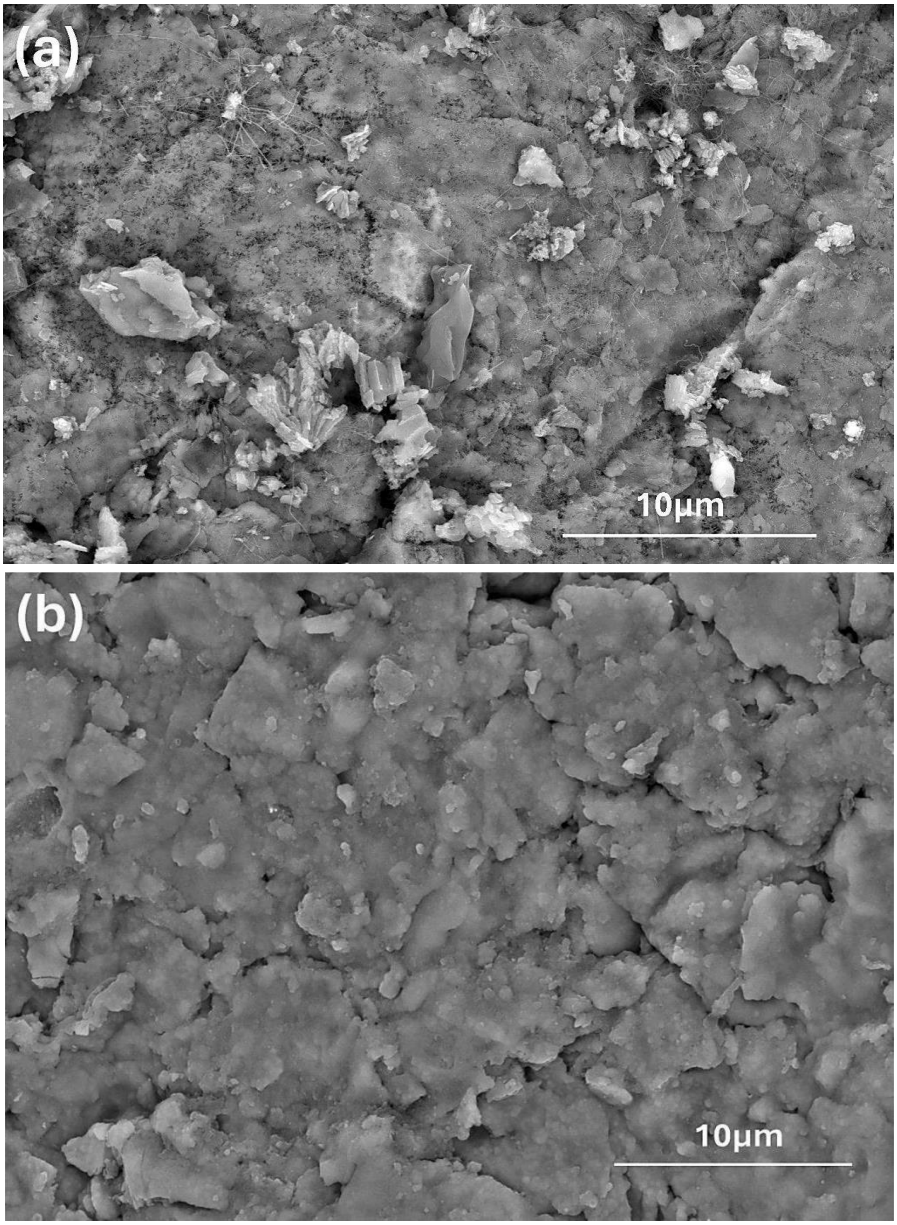

Figure 3. (a) Dispersed HEA particles in 5 wt% composite, and **(b)** Inetwork structure in 30 wt% composite.

Multidisciplinary Materials Chronicles, 2025, Vol. 2, Iss. 1, 92-103
DOI: 10.62184/mmc.jmmc110020254

Research Article

3.2. Thermal properties

Figure 4 shows that thermal expansion behavior is consistent with microstructural evolution relative to the thermal expansion of pure aluminum ($\delta L/L \approx 9.2\times10^{-3}$ at 400 °C); metallic-expansion behavior. The improvement in thermal expansion behavior starts immediately upon the incorporation of HEA, with decreasing (=increasing dimensional stability) response for each incremental amount of HEA. The most significant enhancement, corresponding to $\delta L/L \approx 5.6\times10^{-3}$ at 400°C, is achieved for the HEA composite with 30 wt% of the alloy, marking an impressive increase of ~39% over pure aluminum.

This trend is also supported by CTE values that decrease almost linearly concerning HEA weight fraction (from 22.3 μm/m°C for pure aluminum down to 13.6 μm/m°C at 30 wt% of the constituent HEA). Figure 5 shows that such a systematic decrease is accompanied by microstructural evolution: the increasing volume fraction of HEA particles contributes to forming a stronger thermally stable framework. The universal consistency of CTE reductions in each composition implies a consistent and predictable correlation between HEA content and thermal stability. Several complementary factors have contributed to this mechanism of enhanced thermal stability. The HEA particles are composed of isolating isotropic atomic arrangements, and the nature of thermodynamic behavior makes them expand less than the matrix, making them a good restraining consideration against thermal cycling-induced deformation. Moreover, stable interfaces are the result between pure aluminum and HEA particles that restrain lattice vibration. Hence, it alleviates dimensional change. The gradual change from sparse particle distribution to an interconnected network structure with increasing HEA content further strengthens this stabilizing effect.

These results highlight the design of a thermally stable aluminum composite system with strategic control over HEA content that permits customized thermal expansion properties. The predictable linear correlation between thermal property and composition and systematic microstructural evolution enables a rational design strategy for the further consideration of aluminum-based composites in engineering applications related to heat management.

3.3. Dynamic behavior using Finite Element Method (FEM)

Table 1 presents the fundamental mechanical properties of the Al-HEA composite system across the studied composition range (0-30 wt% HEA). The data shows the theoretical density increasing from 2.7 g/cm³ for pure aluminum to 3.3618 g/cm³ at 30 wt% HEA content. Young's modulus exhibits a corresponding increase from 67.2912 GPa to 89.8805 GPa, while Poisson's ratio values range from 0.3209 to 0.3275. These parameters were implemented in the finite element analysis to characterize the composite behavior.

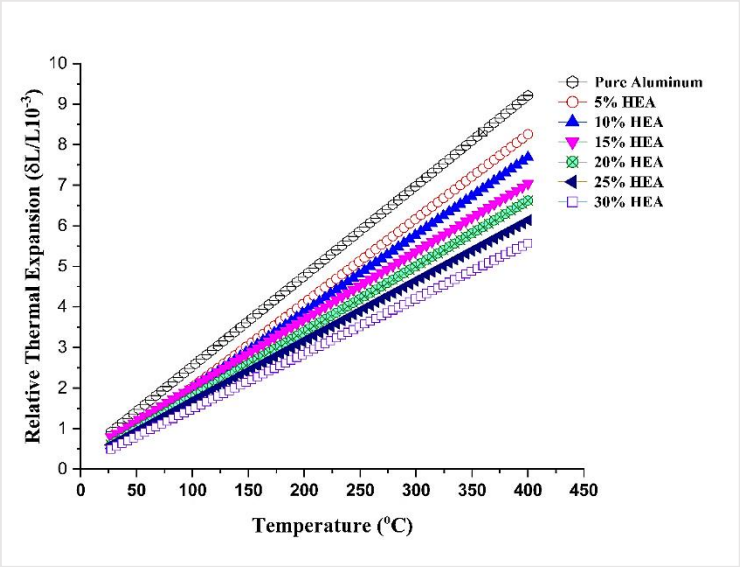

Figure 4. Temperature-dependent relative thermal expansion behavior of Al-HEA composites with varying HEA content (0-30 wt%).

Multidisciplinary Materials Chronicles, 2025, Vol. 2, Iss. 1, 92-103

DOI: 10.62184/mmc.jmmc110020254

Research Article

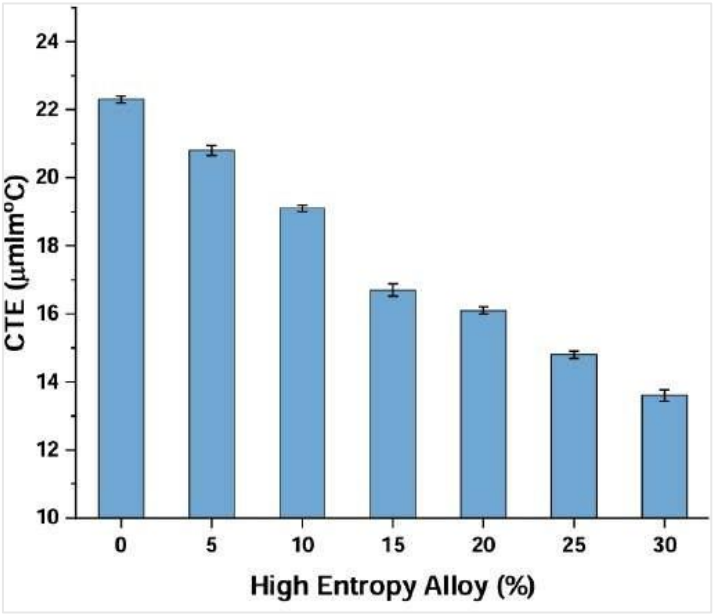

Figure 5. Coefficient of Thermal Expansion (CTE) versus HEA content showing consistent linear reduction with increasing reinforcement content.

Table 1. Mechanical properties of Al-HEA composites as a function of reinforcement content.

HEA%	Density(g/cm^3)	Young's modulus (GPa)	Poisson Ratio
0	2.7	67.2912	0.3209
5	2.7917	70.1261	0.3215
10	2.8895	73.4961	0.3221
15	2.9946	78.4523	0.3238
20	3.1079	81.9409	0.3248
25	3.2299	86.7356	0.3260
30	3.3618	89.8805	0.3275

A modal analysis was conducted using ANSYS software to investigate the dynamic behavior of the composite samples. This finite element analysis tool allows for determining structures' natural frequencies and mode shapes, providing crucial insights into their dynamic characteristics. The analysis involved creating a detailed finite element model of the composite sample, incorporating its geometry, material properties, and boundary conditions. By solving the eigenvalue problem, ANSYS determined the natural frequencies at which the structure resonates and the corresponding mode shapes, representing the characteristic deformation patterns. This modal analysis provides a foundation for understanding the dynamic response and stability of the composite samples under various loading conditions, as demonstrated by the findings in Figure 6. Modal analyses of a pure aluminum tube provide a look into the complete mechanical behavior characterization data using finite element methods. In natural frequency analysis, the first mode shape has a maximum total deformation of 6.0577×10^{-3} m at 2351.3 Hz; the third and fourth mode maximum deformation will be 5.2001×10^{-3} m and 5.8862×10^{-3} m for 7812.7 Hz and 10364 Hz, respectively. These values set a baseline for individual frequencies of pure aluminum structures.

First Mode (2300 Hz): Represents the fundamental frequency of vibration, characterized by the most straightforward deformation pattern where the structure moves in a single primary direction. Third Mode (7800 Hz): Exhibits a more complex vibrational pattern with multiple nodes and antinodes, resulting in higher frequency oscillations. Fourth Mode (10300 Hz): Demonstrates

Multidisciplinary Materials Chronicles, 2025, Vol. 2, Iss. 1, 92-103
DOI: 10.62184/mmc.jmmc110020254

Research Article

the most complex deformation pattern of the three modes analyzed, with additional nodal points and higher frequency vibrations. Figure 7 demonstrates that increasing the amount of High-Entropy Alloy (HEA) in an aluminum tube strengthens it and makes it less prone to vibrations, as shown by the rise in resonance frequencies across three different vibration modes. Specifically, the first mode shows a modest 3% increase in frequency when HEA is increased from 0% to 30%, the third mode shows a more significant 15.4% increase, and the fourth mode exhibits the highest rise at 16.5%. These increases, attributed to the stiffening effect of HEA, suggest improved stability and potential for better performance under dynamic loads, particularly in applications requiring vibration resistance.

3.4. Buckling behavior using Finite Element Method (FEM)

The buckling load, which represents the compressive force a structure can withstand before collapsing, steadily increases with the addition of HEA. Pure aluminum exhibits a buckling load of 0.497 N. This value progressively rises with increasing HEA content, reaching 0.66404 N at 30% HEA. This trend indicates that including HEA significantly enhances the structural integrity and stability of the aluminum, making it more resistant to buckling failure. The increasing buckling load suggests that the HEA reinforces the pure aluminum, effectively hindering its deformation under compressive forces. Figure 8 illustrates that the pure aluminum tube (0% HEA) exhibits characteristic resonance frequencies of around 2300 Hz, 7800 Hz, and 10300 Hz for the first, third, and fourth modes, respectively. The steady frequency increase upon adding HEA signifies a gradual enhancement of the structure's stability. Eigenvalue buckling analysis in Figure 8 indicates the buckling load characteristics with eigenvalues, where the pure aluminum structure presents the initial buckling resistance value of 0.50 N. The gradual rate to 0.66 N with rising HEA content indicates the superior support effect for the structure. The maximum buckling load multiplier is 4.97e+005, and the corresponding deformation shows the typical mode shape under buckling.

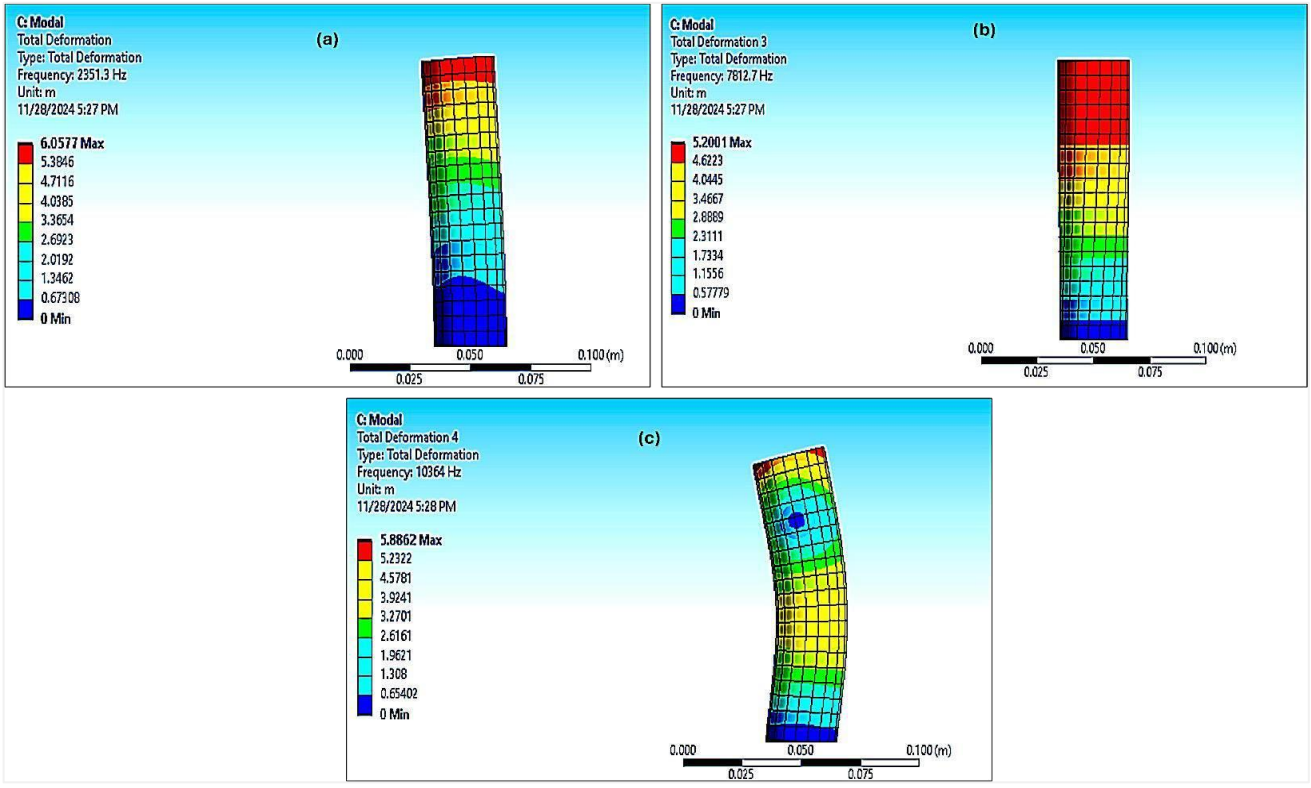

Figure 6. Mode shapes and total deformation distributions from finite element modal analysis of the aluminum tube: **(a)** First mode shape at 2351.3 Hz showing maximum deformation of 6.0577×10^{-3} m, **(b)** Third mode shape at 7812.7 Hz with maximum deformation of 5.2001×10^{-3} m, and **(c)** Fourth mode shape at 10364 Hz exhibiting maximum deformation of 5.8862×10^{-3} m.

Multidisciplinary Materials Chronicles, 2025, Vol. 2, Iss. 1, 92-103

DOI: 10.62184/mmc.jmmc110020254

Research Article

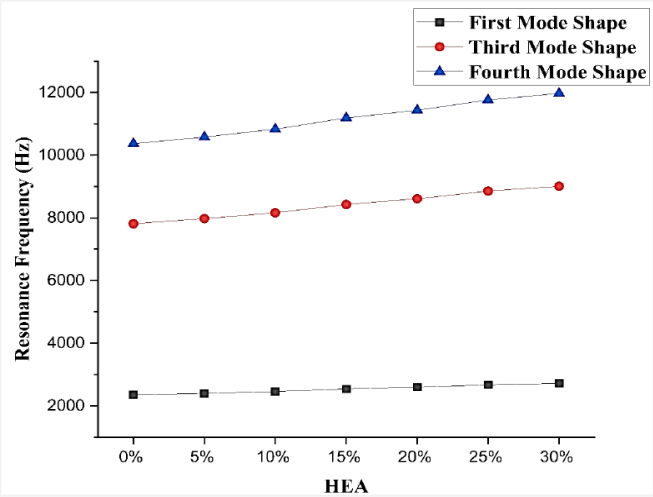

Figure 7. Effect of HEA content (0-30 wt%) on the resonance frequencies of aluminum-based composites for the first, third, and fourth mode shapes.

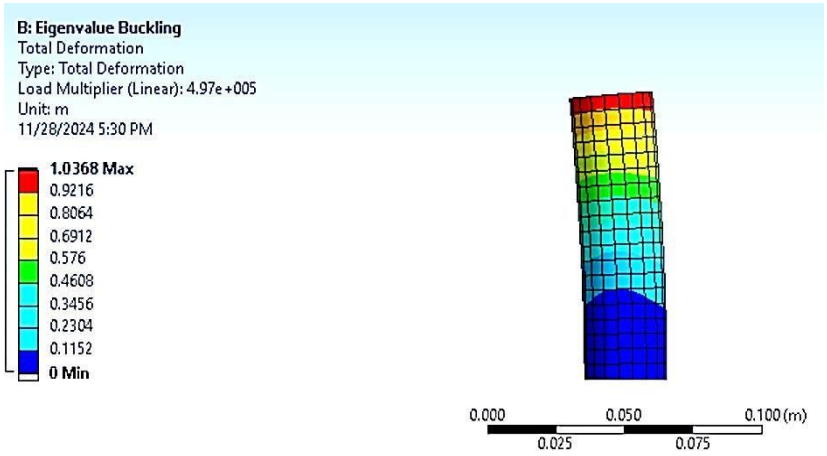

Figure 8. The Eigenvalue buckling analysis of the aluminum tube shows the total deformation distribution.

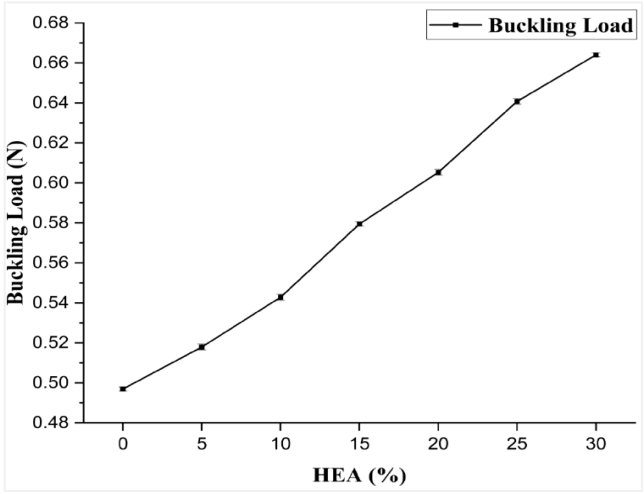

Figure 9. The graph shows a systematic increase in buckling load with increasing HEA content from 0 to 30 wt%.

DOI: 10.62184/mmc.jmmc110020254

The simulation findings provide a solid foundation for assessing the impact of HEA additions on the aluminum structure's dynamic and static mechanical characteristics. Figure 9 clarifies the correlation between the mode of deformation and the basic buckling resistance, providing insights into evaluating the structural integrity of pure aluminum and its enhancement potential with the inclusion of HEAS.

Adding HEA to aluminum creates a composite with significantly improved stability and buckling resistance. As HEA content increases from 0% to 30%, resonance frequencies steadily rise, indicating a stiffer structure less prone to vibrations. This is supported by the increase in buckling load from 0.50 N for pure aluminum to 0.66 N with 30% HEA, demonstrating enhanced strength and resistance to collapse under pressure. This synergy between aluminum and HEA, likely due to the HEA's complex microstructure, results in a material well-suited for dynamic loading conditions, making it a promising candidate for applications like aerospace components and automotive parts where lightweight and high strength are critical.

Triplicate samples were prepared and tested for each HEA concentration (0-30 wt%). One-way Analysis of Variance ANOVA revealed statistically significant differences in buckling load across HEA concentrations ($F(6,14) = 1562.33$, $p < 0.0001$). Post-hoc Tukey's test confirmed significant differences between all HEA concentrations, with systematic increases in buckling load corresponding to higher HEA content. The maximum buckling load (0.664 ± 0.001 N) was achieved at 30 wt% HEA, representing a 33.6% increase compared to pure aluminum (0.497 ± 0.001 N).

The research confirmed the successful incorporation of the emulsified reinforcing phase of Fe-Co-Ni-Cr-Mo high entropy alloy into the pure aluminum, significantly improving the thermal and mechanical behaviors of the composites produced. The systematic correlation between HEA content and material performance is demonstrated by the 39% decrease in thermal expansion coefficient and the corresponding increase in structural stability, manifested by modal and buckling analyses. This transition from the initial dispersed distribution of building blocks to an increasingly interconnected network structure focuses on the mechanistic insight behind the reinforcement process. Such a quantitative basis will enable the tailored development of aluminum-based composites with desirable properties for advanced thermal management applications and pave new pathways in advanced materials engineering. The systematic correlations between HEA content and material properties were quantified through rigorous statistical regression analysis of the experimental data. Linear regression models were developed to characterize the relationships between HEA weight percentage (independent variable) and two key dependent variables: coefficient of thermal expansion (CTE) and buckling load. The CTE correlation is expressed as $y = -0.284x + 22.1$ ($R^2 = 0.994$), where y represents CTE in μm/m°C and x represents HEA content in weight percentage. The negative slope coefficient (-0.284) quantifies the rate of CTE reduction with increasing HEA content, while the high coefficient of determination ($R^2 = 0.994$) validates the strong linear relationship. Similarly, the buckling load correlation follows $y = 0.0055x + 0.497$ ($R^2 = 0.998$), where y represents the buckling load in N. The positive slope coefficient (0.0055) indicates the proportional enhancement in mechanical stability with increasing HEA content, supported by an exceptionally high R^2 value of 0.998. Both regression equations demonstrate statistically significant relationships ($p < 0.05$) and provide mathematical models for predicting material properties at any given HEA concentration within the studied range (5-30 wt%). The complementary nature of these correlations - decreasing thermal expansion and increasing mechanical stability- quantitatively validates the synergistic effects achieved through HEA reinforcement of the pure aluminum.

4. Conclusion

The study successfully incorporated a HEA into a pure aluminum matrix, significantly improving thermal and mechanical properties.

- Adding HEA resulted in a 39% reduction in the thermal expansion coefficient. This indicates that the composite material is less prone to dimensional changes due to temperature variations.
- Structural stability was enhanced, as evidenced by modal and buckling analyses. This suggests the composite material is more resistant to vibrations and buckling under load, with the maximum buckling load showing a 33.6% increase at 30 wt% HEA compared to pure aluminum.
- These improvements involve the transition of HEA particles from an initially dispersed distribution to an interconnected network structure. This network effectively reinforces pure

DOI: 10.62184/mmc.jmmc110020254

Research Article

aluminum. The results of this study have practical implications for the development of aluminum-based composites with customized properties suitable for advanced thermal management applications and other engineering uses, including aerospace, electronic cooling systems, automotive components, and industrial manufacturing.

Author information

Corresponding author: Alqasem M. Alsamawi*

E-mail: aahmedmohammedalsamawi@stu.kau.edu.sa

ORCID iD: 0009-0008-5137-5968

References

[1] P.A. Ibrahim, İ. Özkul, C.A. Canbay, An overview of high-entropy alloys, Emerg. Mater. 5 (2022) 1779-1796. https://doi.org/10.1007/s42247-022-00349-z.

[2] N. Kumar Katiyar, K. Biswas, J.-W. Yeh, S. Sharma, C. Sekhar Tiwary, A perspective on the catalysis using the high entropy alloys, Nano Energy 88 (2021) 106261. https://doi.org/10.1016/j.nanoen.2021.106261.

[3] A. Rashidy Ahmady, A. Ekhlasi, A. Nouri, M. Haghbin Nazarpak, P. Gong, A. Solouk, High entropy alloy coatings for biomedical applications: A review, Smart Mater. Manuf. 1 (2023) 100009. https://doi.org/10.1016/j.smmf.2022.100009.

[4] M. Zhang, Y. Tian, X. Zheng, Y. Zhang, L. Chen, J. Wang, Research progress on multi- component alloying and heat treatment of high strength and toughness Al-Si-Cu-Mg cast aluminum alloys, Materials. 16 (2023) 1065. https://doi.org/10.3390/ma16031065.

[5] Z. Niu, G. Liu, T. Li, S. Ji, Effect of high pressure die casting on the castability, defects and mechanical properties of aluminum alloys in extra-large thin-wall castings, J. Mater. Process. Technol. 303 (2022) 117525. https://doi.org/10.1016/j.jmatprotec.2022.117525.

[6] S.C. Altıparmak, V.A. Yardley, Z. Shi, J. Lin, Challenges in additive manufacturing of high- strength aluminum alloys and current developments in hybrid additive manufacturing, Int. J. Lightweight Mater. Manuf. 4 (2021) 246-261. https://doi.org/10.1016/j.ijlmm.2020.12.004.

[7] T. Sonar, M. Ivanov, E. Trofimov, A. Tingaev, I. Suleymanova, An overview of microstructure, mechanical properties, and processing of high entropy alloys and its future perspectives in aero-engine applications, Mater. Sci. Energy Technol. 7 (2024) 35-60. https://doi.org/10.1016/j.mset.2023.07.004.

[8] S.A. Kareem, J.U. Anaele, E.O. Aikulola, U.S. Anamu, A. Koko, M.O. Bodunrin, K.K. Alaneme, Aluminium matrix composites reinforced with high entropy alloys: A comprehensive review on interfacial reactions, mechanical, corrosion, and tribological characteristics, J. Mater. Res. Technol. 30 (2024) 8161-8186. https://doi.org/10.1016/j.jmrt.2024.05.153.

[9] C. Han, Q. Fang, Y. Shi, S.B. Tor, C.K. Chua, K. Zhou, Recent advances on high-entropy alloys for 3D printing, Adv. Mater. 32 (2020) 1903855. https://doi.org/10.1002/adma.201903855.

[10] I. Basu, J.T.M. De Hosson, Strengthening mechanisms in high entropy alloys: Fundamental issues, Scr. Mater. 187 (2020) 148-156. https://doi.org/10.1016/j.scriptamat.2020.06.019.

[11] Y. Yuan, J.J. Wang, J. Wei, W.Y. Chen, H.L. Yan, N. Jia, Cu alloying enables superior strength-ductility combination and high corrosion resistance of FeMnCoCr high entropy alloy, J. Alloys Compd. 970 (2024) 172543. https://doi.org/10.1016/j.jallcom.2023.172543.

[12] X. Yan, P.K. Liaw, Y. Zhang, Order and disorder in amorphous and high-Entropy Materials, Metall. Mater. Trans. 52 (2021) 2111-2122. https://doi.org/10.1007/s11661-021-06250-4.

[13] B. Kang, S. Lee, W. Lee, K.N. Yoon, E.S. Park, H. Jang, Review on thermal transport and lattice dynamics of high-entropy alloys containing Ni, Curr. Opin. Solid State Mater. Sci. 29 (2024) 101146. https://doi.org/10.1016/j.cossms.2024.101146.

[14] Z. Sun, C. Shi, L. Gao, S. Lin, W. Li, Thermal physical properties of high entropy alloy Al0.3CoCrFeNi at elevated temperatures, J. Alloys Compd. 901 (2022) 163554. https://doi.org/10.1016/j.jallcom.2021.163554.

[15] X. Yin, C.S. Tang, Y. Zheng, J. Gao, J. Wu, H. Zhang, M. Chhowalla, W. Chen, A.T.S. Wee, Recent developments in 2D transition metal dichalcogenides: phase transition and applications of the (quasi-)metallic phases, Chem. Soc. Rev. 50 (2021) 10087-10115. https://doi.org/10.1039/D1CS00236H.

[16] T. Xin, S. Tang, F. Ji, L. Cui, B. He, X. Lin, X. Tian, H. Hou, Y. Zhao, M. Ferry, Phase transformations in an ultralight BCC Mg alloy during anisothermal aging, Acta Mater. 239 (2022) 118248. https://doi.org/10.1016/j.actamat.2022.118248.

DOI: 10.62184/mmc.jmmc110020254

Research Article

[17] S. Abdollahramezani, O. Hemmatyar, M. Taghinejad, H. Taghinejad, A. Krasnok, A.A. Eftekhar, C. Teichrib, S. Deshmukh, M.A. El-Sayed, E. Pop, M. Wuttig, A. Alù, W. Cai, A. Adibi, Electrically driven reprogrammable phase-change metasurface reaching 80% efficiency, Nat. Commun. 13 (2022) 1696. https://doi.org/10.1038/s41467-022-29374-6.

[18] V. Mohammad-Hosseini, G. Rezaei, H. Raanaei, B. Vaseghi, S. Kamali, Structural, magnetic, and thermal properties of nanocrystalline $(Fe_{55}Cu_{20}Al_{25})_{90}B_{10}$ alloy processed by mechanical alloying, Mater. Chem. Phys. 323 (2024) 129671. https://doi.org/10.1016/j.matchemphys.2024.129671.

[19] D. Kumar, R. Seetharam, K. Ponappa, A review on microstructures, mechanical properties and processing of high entropy alloys reinforced composite materials, J. Alloys Compd. 972 (2024) 172732. https://doi.org/10.1016/j.jallcom.2023.172732.

[20] Y. Xiong, F. Zhang, Y. Huang, C. Shang, Q. Wan, Multiple strengthening via high-entropy alloy particle addition in titanium matrix composites fabricated by spark plasma sintering, Mater. Sci. Eng. A 859 (2022) 144235. https://doi.org/10.1016/j.msea.2022.144235.

[21] C. Zhang, J. Zhu, C. Ji, Y. Guo, R. Fang, S. Mei, S. Liu, Laser powder bed fusion of high- entropy alloy particle-reinforced stainless steel with enhanced strength, ductility, and corrosion resistance, Mater. Des. 209 (2021) 109950. https://doi.org/10.1016/j.matdes.2021.109950.

[22] C. Gao, Q. Wang, M. Wei, H. Fan, L. Zhao, Y. Wei, Q. Ma, Effects of reinforcement volume fraction on mechanical properties and microstructures of 7075Al matrix composites reinforced by FeCoCrNiAl high-entropy alloy particles, Metals 12 (2022) 851. https://doi.org/10.3390/met12050851.

[23] L.D. Hung Anh, Z. Pásztory, An overview of factors influencing thermal conductivity of building insulation materials, J. Build. Eng. 44 (2021) 102604. https://doi.org/10.1016/j.jobe.2021.102604.

[24] A. Rajan, M. Sharma, N.K. Sahu, Assessing magnetic and inductive thermal properties of various surfactants functionalized Fe_3O_4 nanoparticles for hyperthermia, Sci. Rep. 10 (2020) 15045. https://doi.org/10.1038/s41598-020-71703-6.

[25] Y. Ouyang, L. Bai, H. Tian, X. Li, F. Yuan, Recent progress of thermally conductive polymer composites: Al_2O_3 fillers, properties and applications, Compos. Part A Appl. Sci. Manuf. 152 (2022) 106685. https://doi.org/10.1016/j.compositesa.2021.106685.

[26] Q. Chen, M. Yu, K. Cao, H. Chen, Thermal conductivity and wear resistance of cold sprayed Cu-ceramic phase composite coating, Surf. Coat. Technol. 434 (2022) 128135. https://doi.org/10.1016/j.surfcoat.2022.128135.

[27] O. Eseonu, M. Mactier, E. Ferguson, F. Quondamatteo, M. Blyth, B. Jones, Soft-tissue landmarks for tibial baseplate rotational alignment in total knee arthroplasty: A cadaveric study, Clin. Anat. 35 (2022) 1107-1113. https://doi.org/10.1002/ca.23921.

[28] Y. Ouyang, F. Ding, L. Bai, X. Li, G. Hou, J. Fan, F. Yuan, Design of network Al_2O_3 spheres for significantly enhanced thermal conductivity of polymer composites, Compos. Part A Appl. Sci. Manuf. 128 (2020) 105673. https://doi.org/10.1016/j.compositesa.2019.105673.